Journal of Environmental Chemical Engineering 13 (2025) 115795

Contents lists available at ScienceDirect

Journal of Environmental Chemical Engineering

journal homepage: www.elsevier.com/locate/jece

Advancing the enzymatic removal of antibiotics with unspecific peroxygenase and vanadium chloroperoxidase

Sabrina de Boer [a,b,*], Daniel Sastre [a], Aly Castillo [c,d], Sabela Balboa Méndez [a], Frank Hollmann [e], Marta Lores [f], Andreas Schäffer [b], María Teresa Moreira [a]

[a] CRETUS, Department of Chemical Engineering, Universidade de Santiago de Compostela, Santiago de Compostela 15782, Spain
[b] Institute for Environmental Research, RWTH Aachen University, Worringerweg 1, Aachen 52074, Germany
[c] i-Grape Laboratory, Via Isaac Peral 32, Santiago de Compostela 15890, Spain
[d] CRETUS, Department of Analytical Chemistry, Nutrition, and Food Science, Universidade de Santiago de Compostela, Santiago de Compostela, Spain
[e] Department of Biotechnology, Delft University of Technology, Delft 2629 Hz, The Netherlands
[f] LIDSA, Department of Analytical Chemistry, Nutrition and Food Science, Universidade de Santiago de Compostela, Santiago de Compostela 15782, Spain

ARTICLE INFO

Keywords:
Oxidoreductases
Watchlist antibiotics
Antibiotic susceptibility
N-oxidation
Advanced wastewater treatment

ABSTRACT

Enzymatic processes for the remediation of wastewater containing organic pollutants are a promising alternative to advanced treatment processes that are often energy intensive and/or generate waste or by-products. For antibiotics, enzyme systems studied to date have been limited by substrate scope, pH tolerance, and stability. In this work, the remediation potential of two promiscuous H_2O_2-dependent enzymes is explored: the unspecific peroxygenase from *Agrocybe aegerita* (*Aae*UPO) and the chloroperoxidase from *Curvularia inaequalis* (*Ci*VCPO), for the removal of four antibiotics commonly found in WWTP effluents and surface waters. While both enzymes showed a high removal potential for sulfamethoxazole (SMX) as a model antibiotic, *Ci*VCPO was inactive in municipal wastewater, likely due to the presence of phosphate and nitrate. In contrast, *Aae*UPO remained active and stable within a suitable pH and temperature range. The transformation products showed decreased antibiotic activity against a susceptible strain of *E. coli* and decreased phytotoxicity, as indicated by the increased root length of *Daucus carota*. Peroxygenases are known to be sensitive to excess H_2O_2, and *Aae*UPO displays significant catalase activity at low substrate concentrations. To minimise H_2O_2-mediated inactivation, experiments were conducted at various H_2O_2 dosing rates in batch mode. Optimal conditions for the operation of a continuous enzymatic membrane reactor were then investigated, achieving over 95 % removal of SMX. This lays the groundwork for continuous operation and paves the way for efficient reactor design.

1. Introduction

To ensure the availability and quality of freshwater, a resource under increasing pressure, improved water management strategies must be implemented [1]. A key aspect is the efficient removal of recalcitrant and persistent compounds in wastewater treatment plants (WWTPs) [2]. Although conventional WWTPs are effective at reducing the organic load and nutrient content of wastewater, they largely fail to remove low molecular weight organic pollutants [3]. As a result, these compounds are discharged into natural waters and pose a risk to aquatic life. Antibiotics are of particular concern. Although their concentrations in waters downstream of WWTPs are typically below the minimum inhibitory concentration for acute effects, their presence can exert selective pressure favouring the emergence of antimicrobial resistance genes [4,5].

Source control strategies are challenging to implement due to the essential role of antibiotics in healthcare and the fact that a significant proportion (50–80 %) of administered antibiotics are excreted unchanged [6]. Therefore, reducing antibiotic levels in surface waters can only be effectively achieved through end-of-pipe strategies, such as the

Abbreviations: ABTS, 2,2′-Azino-di3-ethylbenzthiazolin-6-sulfonic acid; CIP, Ciprofloxacin; *Ci*VCPO, *Curvularis inaequalis* vanadium chloroperoxidase; CSTR, Continuously stirred tank reactor; MCD, Monochlorodimedone; *Aae*UPO, unspecific peroxygenase *Agrocybe Aegerita*, recombinantly expressed in *Komagataella phaffii* (*Pichia pastoris*), PaDa-1 variant; PEG, Polyethylene glycol; ROS, Reactive oxygen species; SMX, Sulfamethoxazole; TET, Tetracycline; TMP, Trimethoprim; TP, Transformation product.

* Corresponding author at: CRETUS, Department of Chemical Engineering, Universidade de Santiago de Compostela, Santiago de Compostela 15782, Spain.
E-mail address: sabrinarose.deboer@usc.es (S. de Boer).

https://doi.org/10.1016/j.jece.2025.115795
Received 4 October 2024; Received in revised form 30 January 2025; Accepted 13 February 2025
Available online 14 February 2025

introduction of additional treatment stages. Currently, several physical and chemical processes can be used to remove micropollutants [7]; however, these methods face significant drawbacks, including sludge production and the use of chemicals and energy. As a result, environmentally friendly alternatives are gaining importance. Among these, enzymatic processes are considered a promising approach.

Enzymes offer several advantages over conventional processes: they are non-toxic, biobased and biodegradable. In addition, their catalytic activity can be enhanced by genetic engineering. Among the enzymes studied for micropollutant removal, laccases are the most extensively investigated [8,9]. Despite their high stability and relatively low cost, the substrate scope of laccases is limited to activated substrates such as phenols or N-hydroxides [10,11]. Target compounds lacking these functional groups, such as most antibiotics, can only be transformed in the presence of costly and often toxicity-inducing redox mediators [12], highlighting the need for new biocatalysts. In this work, the potential of two enzymes was investigated: the unspecific peroxygenase from *Agrocybe aegerita* (*Aae*UPO, PaDa-1), [13–15] and the vanadium-containing chloroperoxidase from *Curvularia inaequalis* (*Ci*VCPO) [16].

Peroxygenases such as *Aae*UPO are heme-thiolate enzymes that combine the H_2O_2-dependency of peroxidases and the high reactivity of P450 monooxygenases [17,18]. This opens up new possibilities for the conversion of priority pollutants and pharmaceuticals [19,20]. *Aae*UPO has demonstrated activity against sulfamethazine and sulfadiazine [21], but its activity against other antibiotics has yet to be explored. While several studies have elucidated the mechanisms of substrate conversion by *Aae*UPO [22,23], and a continuous reactor has been proposed for the conversion of model substrates ABTS and ethylbenzene [24], wastewater treatment processes at micromolar contaminant concentrations have not yet been investigated.

Similarly, no studies have reported antibiotic removal by *Ci*VCPO. As member of the haloperoxidase family, *Ci*VCPO oxidises halides to the corresponding hypohalites at the expense of H_2O_2 [25]. The reactive hypohalites leave the active site of the enzyme, allowing their interaction with a sterically challenging substrate. Under certain conditions, also singlet oxygen can be formed [26], that can contribute to the oxidative degradation of the target pollutants.

In this work, the removal of four antibiotics was assessed: the sulphonamide sulfamethoxazole (SMX) and its adjuvant trimethoprim (TMP), the fluoroquinolone ciprofloxacin (CIP), and tetracycline hydrochloride (TET) from the tetracycline class. Although penicillins, cephalosporins, and macrolides are the most widely used antibiotics globally [27], they are more susceptible to abiotic and biotic hydrolysis in the environment [28]. Three selected substances—SMX, TMP, and CIP—are or have been considered in the Watch List under the Water Framework Directive [29], while TET is a common substrate in laccase-based removal studies [30].

Besides determining the substrate scope of the two enzymes, their applicability under conditions relevant to wastewater treatment is investigated. Given the known instability of *Aae*UPO in the presence of its cofactor H_2O_2, SMX removal is evaluated in fed-batch and continuous reactors at a laboratory scale. The effectiveness of the proposed enzymatic treatment with *Aae*UPO was assessed not only in terms of the resulting transformation products but also through effect-based assays. Additionally, the impact of mixtures of multiple antibiotics on removal efficiency was studied to highlight the remaining challenges of enzyme-mediated remediation of wastewater pollutants.

2. Materials and methods

2.1. Chemicals

The PaDa-1 variant of *Aae*UPO (UPO 23®) was purchased from EvoEnzyme, Madrid, with a specific activity of 828 U/mg as freeze-dried powder, which was redissolved according to the supplier's instructions. The enzyme solution was aliquoted and stored at −20 °C. Each thawed batch was used for no more than one week and the activity was determined before each experiment. *Ci*VCPO was prepared following literature procedures [31,32], with an activity of 3.9 U/mmol with respect to the monochlorodimedone (MCD) assay. 2,2′-azino-bis(3-ethylbenzothiazoline-6-sulfonic acid (ABTS), purity > 98 % and hydrogen peroxide 30 % were purchased from Merck and stocks were prepared weekly and daily, respectively. The exact concentration of H_2O_2 was determined by titration with potassium permanganate standardized with calcium oxalate. Antibiotic standards were supplied by Merck (Sigma Aldrich), the standard 4-nitro-SMX was supplied by Toronto Research Chemicals.

2.2. Enzymatic activity assays

The activity of *Aae*UPO was determined by the ABTS assay using 2 mM H_2O_2 and 1 mM ABTS in 0.1 M sodium citrate buffer at pH 4. The formation of the $ABTS^{+\cdot}$ radical was monitored for 3 min by reading absorbance at 420 nm. One unit of activity was defined as the formation of 1 μmol/min of $ABTS^{+\cdot}$ considering an extinction coefficient of 36,000 L/(mol cm). The relative activity of *Ci*VCPO was determined by plotting the linear range of bromophenol blue formation from a 40 μM solution of phenol red and 0.1 M KBr in sodium citrate buffer at pH 5.6, the absorbance was read at 592 nm (Fig. S2) [33]. All activity measurements were performed using a HT Biotek Synergi plate reader.

2.3. Screening degradation experiments

Experiments were performed in stirred amber vials ($V_{Reaction}$ = 5 mL), at 22 °C, in buffer and secondary effluent from a municipal wastewater treatment plant (composition summarised in Table S1). The antibiotics of interest were prepared at 1 g/L in MeOH, except for tetracycline, which was dissolved in water. For *Aae*UPO, experiments were performed in potassium phosphate buffer (pH 7; 0.1 M), while for *Ci*VCPO, sodium citrate buffer (0.02 M; pH 5.6) in the presence of 5 mM NaCl was used. The antibiotic concentration was chosen at 5 mg/L to facilitate the identification of transformation products. Unless otherwise stated, for pollutant spiking, the organic solvent was completely evaporated prior to mixing with the water matrix. H_2O_2 was added in a single spike to reach a concentration of 0.2 mM in case of *Aae*UPO (500 U/L, ABTS) and 100 mM in case of *Ci*VCPO (390 U/L, MCD). The following buffers were used for the pH activity experiments of *Aae*UPO: Sodium citrate buffer (0.1 M, pH 3–6), sodium phosphate buffer (0.1 M, pH 6–8), and sodium carbonate buffer (0.1 M, pH 8–9).

2.4. Initial rate experiments

Experiments were performed in stirred amber flasks in 5 mL sodium phosphate buffer (0.1 M, pH 7). The enzyme concentration was adjusted to 500 U/L. Experiments were started by adding 200 μL of H_2O_2, the amount of SMX added was corrected for dilution by H_2O_2. Samples of 300 μL were taken every 10 s and immediately added to 10 μL of 100 mM NaN_3 solution to deactivate the enzyme.

2.5. Fed-batch removal studies

Reactions were performed in 50 mL sodium phosphate buffer (0.1 M, pH 7), and in deionized water in stirred glass beakers. The initial SMX concentration was 3.4 μM. The hydrogen peroxide solution was dosed using a syringe pump (New Era Pump Systems, Inc.), applying flow rates of 1–4 mL/min. Samples were taken periodically to quantify H_2O_2, enzyme activity and SMX concentration. The pH was monitored in selected reactions with a glass electrode coupled to a Crison (USA) GLP-21 digital analyser.

2.6. HPLC reaction monitoring

Samples were injected without further purification into a JASCO XLC HPLC system, equipped with a 311 MD diode array detector. Elution was performed on a Gemini® C-18 column (150 ×4.6 mm; 3 μm) (Phenomenex). To determine the removal of the four selected antibiotics, a gradient elution was performed using 5 % acetonitrile (ACN, mobile phase A) and 95 % water (mobile phase B) for 4 min, followed by increasing the ACN to 50 % for 15 min. After restoring the initial elution conditions, the column was equilibrated under these conditions for 5 min. To resolve the SMX transformation products, elution was performed at 30 °C using isocratic conditions of 40 % acetonitrile (ACN, mobile phase A) and 60 % water with 20 mM (mobile phase B) from 0 to 6 min, a gradient to 60 % mobile phase A and 40 % mobile phase B until 8 min, and a return to the original conditions from 8 to 12 min. An injection volume of 20 or 100 μl was chosen depending on the initial concentrations. Chromatograms were processed using the HP ChromNav® version 2.04.06 software.

2.7. Determination of transformation products by UHPLC-QToF

Samples were filtered through 0.22 μm PTFE filters. Untargeted analysis was performed by ultra-high performance liquid chromatography (Elute UHPLC 1300) coupled to a Compact model quadrupole time-of-flight (QToF) mass spectrometer (Bruker Daltonics). Chromatographic separation was performed using an Intensity Solo C18–2 HPLC column (100 mm × 2,1 mm, 1,8 μm; Bruker Daltonics, Bremen, Germany) and a pre-column, kept at 40 °C. The mass deviation correction was performed by injecting an aqueous solution of NaOH and isopropanol (50:50) with 0.2 % formic acid as the calibrant. Mobile phases (A) and (B) consisted of 0.1 % formic acid and 5 mM ammonium formate in water and methanol, respectively. The elution gradient consisted of 0.1 min 96/4 (A/B) where the calibrant enters, followed by an increasing ramp 81.7/18.3 (1 min); 50/50 (2.5 min) and 0.1/99.9 (14 min to 16 min) until returning to the initial conditions after 16.1 min, maintaining isocratic conditions until the end of the run at 20 min. Samples were acquired in Auto MS/MS mode with positive polarity, using an electrospray ionization (ESI) source detecting mainly pseudomolecular [M+H]+ ions, as reported previously with slight modifications [34]. Briefly, an acquisition rate of 8 Hz in 0.3 s cycles over a voltage range of 5–70 eV and a filtering amplitude of 20–1000 *m/z* was used using Compass HyStar acquisition software. Ion source conditions were as follows: capillary voltage 4500 V, nebulizer pressure 29 psi, drying gas 8 L/min and gas temperature 220 °C.

Statistical analysis of the untargeted search was performed by MetaboScape® software Version 4.0.4 (Build 19) using the T-REX 3D algorithm. For the prediction of molecular formulae, SmartFormula was used, based on the exact mass comparison and the isotopic profile of each compound, with the maximum mass deviation error of 5 mDa and mSigma 50 set as acceptable parameters in all cases. The identifications obtained are validated with the Compound Crawler tool and their structural stability is confirmed with the MetFrag software, which combines the analysis of the *in silico* fragmentation of the possible candidates with the search in the main databases (ChemSpider, ChEBI, PubChem) and the use of spectral libraries: Mass Bank European and MassBank of North America (MoNA) and National Center for Biotechnology Information (NCBI). The SMX transformation product 4-Nitro-SMX was further confirmed to have the same elution profile than the purchased standard.

2.8. Quantification of hydrogen peroxide

In the reaction mixtures, hydrogen peroxide was quantified photometrically using an enzymatic method or the FOX assay. For the enzymatic method, ABTS was used as substrate in the presence of an excess of *Aae*UPO, and the end-point absorbance was determined at a wavelength of 418 nm after 5 min incubation (LOD of 8 μM and LOQ of 25 μM, Fig. S3). For lower concentrations, the original FOX assay protocol was adapted for measurement in the microplate reader. The reagent solution contained 0.1 mM xylenol orange, 0.25 mM ammonium iron (II) sulphate, 25 mM H_2SO_4 and 100 mM sorbitol as signal enhancer, as previously described [35]. For the assay, 285 μL of sample solution and 15 μL of the reagent solution were mixed per well, and the absorbance at 560 nm was read after 30 min incubation together with a calibration series. The LOD and LOQ were 0.1 and 0.3 μM, respectively (Fig. S3).

2.9. Continuous reactor setups

A continuously stirred enzymatic membrane reactor (EMR) was set up using a commercial Amicon® cell (V = 240 mL) connected to a feed reservoir with no air headspace (Fig. S9) [36]. The feed was supplied by a Masterflex L/S® peristaltic pump (Cole Parmer) regulated by a Masterflex L/S modular controller. Ultracel® 10 kDa regenerated cellulose ultrafiltration discs (Ø 63.5 mm) were used as the separation membrane and were handled according to the recommendations of the supplier (Merck Millipore). The pressure was kept below 13 psi, which allowed a stable flow rate of 2.5 ± 0.1 mL/min. The residence time distribution was determined by following the increase in conductivity in the effluent after a sudden increase in NaCl concentration in the feed from 0 to 1 g/L (Fig. S10).

2.10. Effect-based assays

2.10.1. Antibiotic susceptibility

In a preliminary screening step, bacteria with a high susceptibility to SMX were selected based on disk diffusion tests, considering the following strains: *Escherichia coli K12, Acinetobacter baumanii M1.50, Streptococcus pneumoniae CECT 769* and *Klebsiella pneumoniae H1.69*. From these strains, *E. coli* and *K. pneumoniae* showed highest susceptibility and were selected for broth dilution assays. Stocks consisted in an aqueous solution of 100 mg/L SMX and the correspondingly concentrated effluent from the continuous reactor. 15 μL of the stock were mixed with 135 μL of Mueller-Hinton Broth containing a 1:100 dilution of the overnight culture of the bacteria. Growth was monitored in triplicates in 96-well U bottom shaped plates for 24 h at 37 °C reading the optical density at 600 nm (OD_{600}).

2.10.2. Seed germination

Seed germination was assessed following the procedure of Hillis et al. with some modifications [6]. Forty *Daucus carota* seeds were placed on a filter paper in a petri dish (Ø = 9 cm) containing 5 mL of the sample diluted in distilled water. A blank was performed in distilled water only. Dishes were sealed with Parafilm® and incubated in the dark at 22 ± 2 °C. Growth was monitored at 4, 7 and 9 days after the start of the experiment. Total length (sum of shoot and root length) was evaluated by manual tracing of backlit photographs of the plates with the software ImageJ (version 1.53.k) [37]. Data was tested for normality and homoscedasticity by the Shapiro-Wilk and the Levene test, respectively. Analysis of variance was performed by Welch-ANOVA and Games-Howell pairwise comparison as post-hoc test. All data analysis was performed with the software OriginPro 2024.

3. Results and discussion

3.1. Conversion of target antibiotics

In a first step, the elimination potential of the two oxidoreductases was determined for the four selected antibiotics (Fig. 1). Therefore, suitable buffered conditions were selected that would guarantee high enzyme activity. While *Aae*UPO shows highest activity for most substrates at pH values close to 7, *Ci*VCPO requires slightly acidic conditions, the presence of halide ions, and absence of phosphate. Preliminary

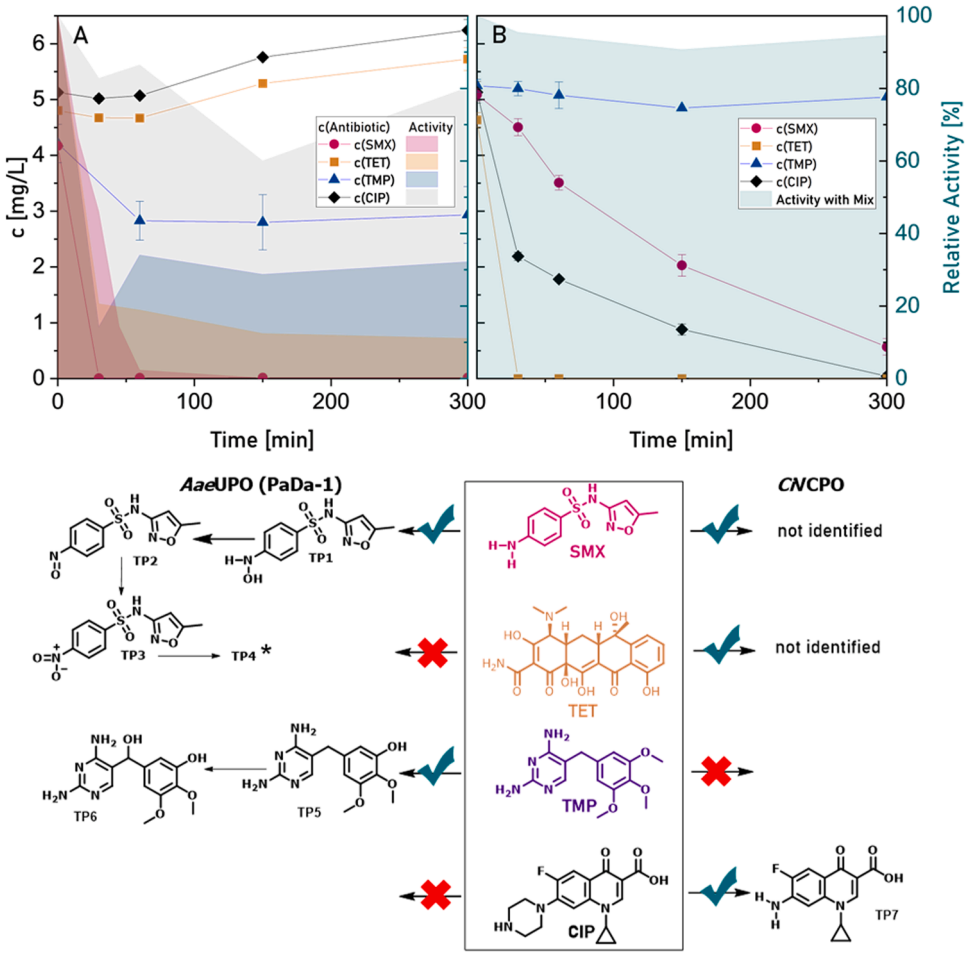

Fig. 1. Model antibiotics used and their conversion by *Aae*UPO and *Ci*VCPO at pH 7 and pH 5.6, respectively (see Section 2.3 for further details). The upper graphs illustrate the removal time course (line graphs) together with the residual enzyme activity (shaded areas), while the lower panel shows the structure of the tentative transformation products. For *Aae*UPO, each antibiotic was degraded individually, while *Ci*VCPO acted on the antibiotic mix. All removal batch experiments were conducted in triplicate.

experiments confirmed that the selected antibiotics were stable in the reaction matrix in the absence of the respective enzymes. This is attributable to the relatively low reactivity of H_2O_2 toward organic compounds in the absence of promotors [38]. In wastewater treatment applications, H_2O_2 is typically applied in combination with UV-C light, (photo)catalysts, or electrochemical processes to enhance the formation of reactive oxygen species, e.g. by disproportionation into hydroxyl radicals.

Comparing the removal of the four antibiotics in presence of *Aae*UPO (Fig. 1A) and *Ci*VCPO (Fig. 1B), the substrate scope of the two enzymes was somewhat complementary, with *Aae*UPO being active on SMX and TMP while *Ci*VCPO converted CIP, TET and SMX. The higher steric demand of CIP and TET may account for the poor conversion by *Aae*UPO, where binding to the active site is a prerequisite for conversion. This is not the case with *Ci*VCPO, which primarily forms hypochlorite which then leaves the enzyme active site. At the selected conditions, in the presence of excess H_2O_2, OCl^- mediates the oxidation of H_2O_2 to $^1O_2$ [39], also indicated by the formation of gas bubbles during the removal experiments. In case of CIP, UHPLC-QToF confirmed cleavage of the piperazine ring (Fig. 1). Similarly, the $^1O_2$-mediated of structurally related norfloxacin had also been reported to proceed via piperazine ring cleavage [40]. However, the reason for the recalcitrance of TMP remains to be elucidated. It has been previously reported that the reaction of TMP with $^1O_2$ is slow and inefficient compared to other oxidative removal pathways [41,42]. Unfortunately, the transformation products of SMX and TET could not be identified to confirm the assumption that no chlorinated by-products are formed under the selected conditions.

In case of *Aae*UPO, the concentration increase of SMX and CIP (Fig. 1A) may have been caused by partial evaporation of the matrix during the experiment. Nevertheless, results from triplicate experiments confirm that the enzyme did not degrade these compounds. TMP-conversion could be attributed to primarily oxidative demethylation of the methoxy substituents and, to some extent, benzylic hydroxylation (Fig. 1). This is in line with the catalytic scope of *Aae*UPO [43–45]. The three transformation products observed in the case of SMX indicate a successive N-oxidation to the corresponding nitro group (Fig. 1). While N-oxidation has been reported for manganese peroxidase and chloroperoxidases [46,47], peroxygenases have mainly shown N-oxidation of pyridine derivatives [48]. Very recently, additional pathways and substrates for *Aae*UPO-catalysed N-oxidations have been reported [49].

Since SMX was converted by both enzymes, their SMX-conversion performance under realistic conditions, i.e. in a municipal WWTP effluent, was further investigated (Fig. 2A and B). Interestingly, *Aae*UPO performed well but with *Ci*VCPO no conversion was observed. A potentially too low chloride concentration was ruled out to explain the apparent inactivity, as shown in an experiment with supplementation of 5 mM NaCl. *Ci*VCPO was not inactivated (Fig. 2B, shaded area). Possibly, phosphate inhibition [50] (the phosphate concentration of the selected wastewater was 4.6 mg/L; 49 μM, Table S1) played a role. The presence of nitrate (8.9 mg/L (0.14 mM) in the effluent may also have contributed to the enzyme inhibition [51]. Further studies are needed to

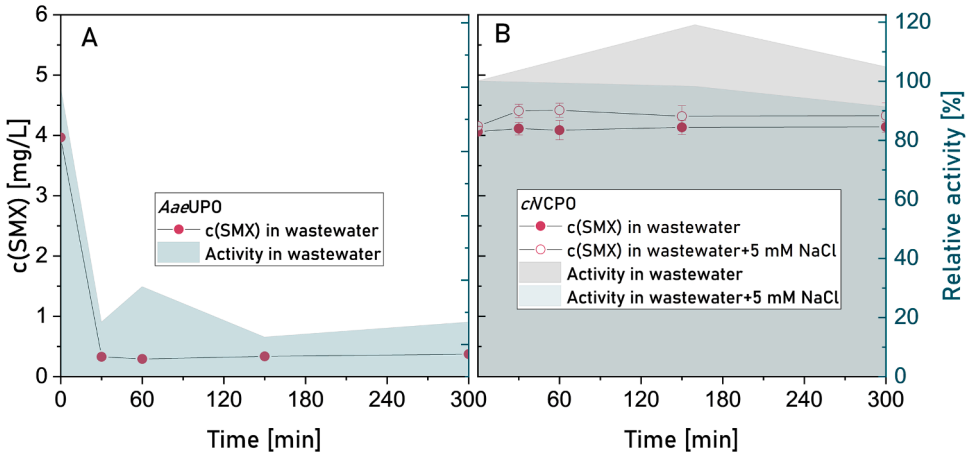

Fig. 2. Time course of removal of antibiotics by *Aae*UPO (A) and *Ci*VCPO (B) in municipal WWTP effluent (pH 6.9). In case of *Ci*VCPO, the removal was also evaluated in an effluent that was supplemented with 5 mM NaCl. Residual enzyme activity is indicated by shaded areas. Experiments were conducted in triplicate.

fully understand the apparent inhibition of *Ci*VCPO in different types of wastewater. Despite the fast removal of SMX achieved with *Aae*UPO, its stability dropped considerably under the applied conditions, requiring a further optimization of the reaction conditions.

3.2. Evaluation of process window for SMX removal by AaeUPO

Municipal wastewater is characterised by a pH range between 7 and 8.5 and temperature typically below 25 °C [52,53]. From an application point-of-view it is important that these conditions match the biocatalyst requirements for high activity and stability. Fig. 3A displays the initial SMX conversion rate of *Aae*UPO, as well as its stability at pH values between 3 and 9. Compared to laccases, which generally exhibit maximal activity at pH 3–5 for most substrates, the maximal rate of SMX conversion by *Aae*UPO was achieved at pH 5.5. Nevertheless, even at pH 8, at least one-third of the maximal rate was achieved. Additionally, the enzyme stability was highest between pH 5 and 7, which is an acceptable range for wastewater treatment applications.

Not surprisingly, the initial rates of SMX removal also exponentially increased with reaction temperature (Fig. 3B). An Arrhenius fit (Fig. S4) yielded an activation energy (E_A) of 50 ± 6 kJ/mol, comparable with previously determined activation energies [54,55]. Moreover, the stability of *Aae*UPO decreased with increasing temperature, in concordance with previous works [13]. However, at temperatures below 25 °C, that are typical for wastewater, the stability appeared reasonably high.

3.3. Interaction of the reacting species

While single pulse dosing of H_2O_2 offers advantages in handling, especially in microliter-scale screening studies [56], the concentrations selected are often not optimized to achieve the maximum removal potential of the enzyme. Although H_2O_2 is an essential cofactor to activate the catalytic site of the enzyme, many peroxide-dependent enzymes are deactivated upon its presence in excess [57]. Monitoring of all reacting species during the sequential addition of *Aae*UPO and H_2O_2 illustrates the ambivalent influence of H_2O_2 concentration on substrate conversion and enzyme stability (Fig. 4).

Substrate conversion by *Aae*UPO occurs either by peroxygenase or peroxidase-like pathways after reactive compound I is formed by H_2O_2 binding and water release. Already in the first phase all initial SMX was consumed and hydroxylamine (TP1), nitroso (TP2) and nitro (TP3) intermediates were detectable (Fig. 4A and B). However, *Aae*UPO had already been inactivated within 30 minutes, while H_2O_2 remained at a concentration of 50 µM. The next dose of active enzyme completed the transformation into TP3 with some traces of a yet undefined further intermediate (TP4) was observed. The concentration of TP3 did not vary significantly upon further addition of *Aae*UPO and H_2O_2. The immediate decrease of the H_2O_2 concentration upon addition of a third pulse of enzyme after completion of substrate conversion illustrates the catalase activity of the enzyme when, in the absence of other substrates, Compound I binds an additional H_2O_2 molecule that is converted to O_2 and

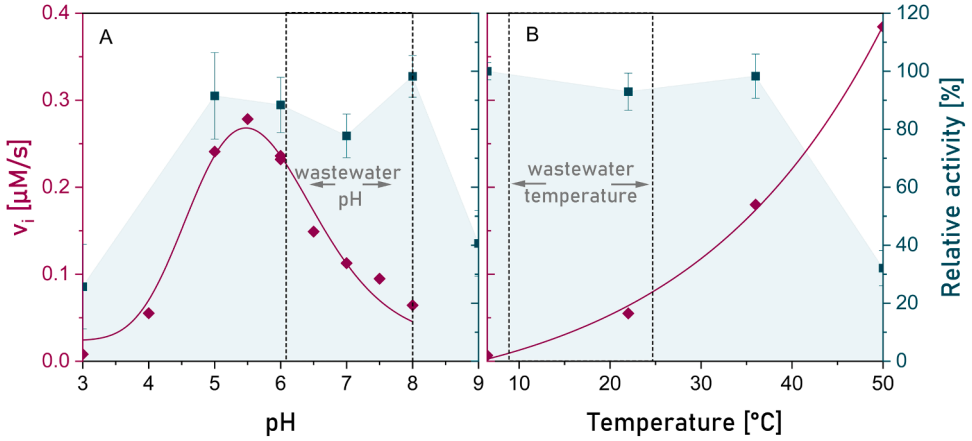

Fig. 3. A) Influence of pH on initial rate of SMX removal (purple) and residual activity after 8 h incubation (green) B) Influence of temperature on initial rate of SMX removal (blue) and residual activity after 3 h of incubation (green). Conditions: 900 µg/L SMX; 0.2 mM H_2O_2; 500 U/L *Aae*UPO. All experiments were performed in triplicate.

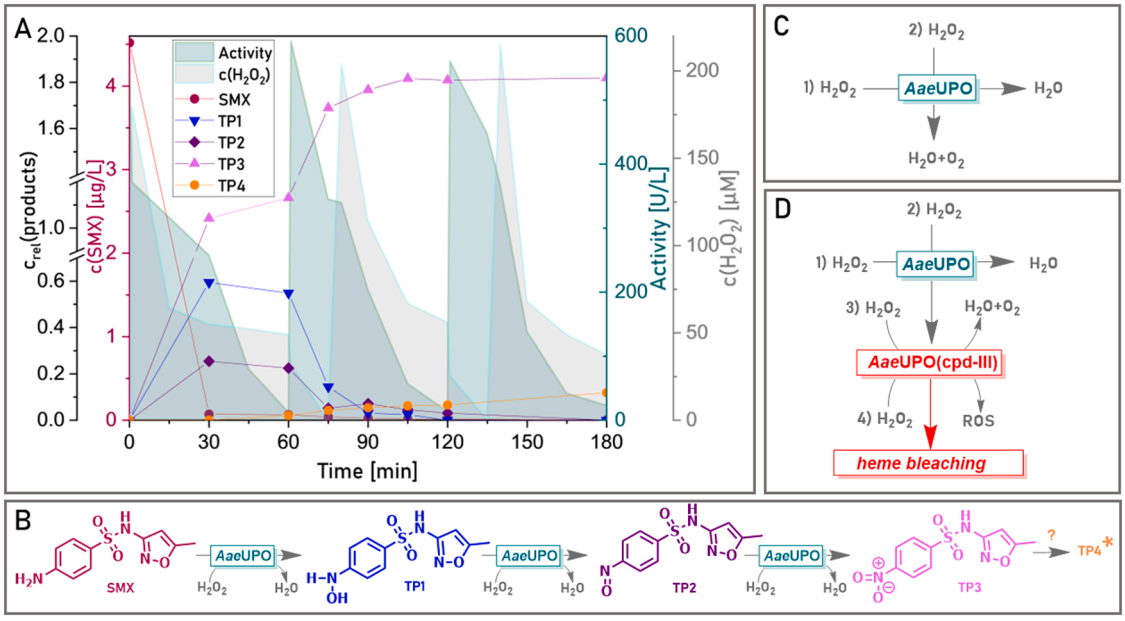

Fig. 4. A) Sequential addition of *Aae*UPO and hydrogen peroxide to achieve complete removal of SMX (red). Transformation products: TP1 (blue); TP2 (dark purple), TP3 (violet), TP4 (orange) were determined relative to the SMX standard. The grey shaded area depicts the residual H_2O_2 concentration, and the green shaded area represents the residual *Aae*UPO activity B) Tentative reaction sequence from SMX to TP4 C) Catalase reaction scheme D) Catalase malfunction reaction scheme.

water upon restoration of the resting state (Fig. 4C) [22]. This pathway is however prone to a malfunction (Fig. 4D) initiated by the binding of a third H_2O_2 molecule to yield the reduced compound III and ultimately leading to the destruction of the catalytic site ("heme bleaching"), potentially by reactive oxygen species (ROS) formed by the reaction of Compound III with additional H_2O_2 molecules [22]. This mechanism is likely to be the main reason for the fast enzyme deactivation and shows the need for a more adequate H_2O_2 dosing strategy.

3.4. Process optimisation in fed batch mode

To further understand the *Aae*UPO-catalysed SMX-conversion, the Michaelis-Menten parameters for both substrates were estimated by initial rate experiments (Fig. S7). The K_M value for SMX was 62 µM. For H_2O_2, an apparent K_M value of about 23 µM was determined with a pronounced substrate inhibition, which can be attributed to the oxidative inactivation of *Aae*UPO. To mimic the intended continuous process conditions, the apparent rate dependence was also determined at different H_2O_2-dosing rates (Fig. 5). The SMX conversion rate increased with the H_2O_2-dosing rate in a saturation-type behaviour similar to classical Michaelis-Menten kinetics. As a result, the SMX conversion rate did not increase linearly with increasing H_2O_2 supply rate. However, since H_2O_2 accumulation was not observed as long as active enzyme was present, this difference can be attributed to an increasing catalase activity of *Aae*UPO, additionally giving rise to an increasing enzyme deactivation by the catalase malfunction pathway. Consequently, at the selected SMX concentration, hydrogen peroxide dosing rates > 15 µM/h should be avoided to prevent inefficient use of H_2O_2 and excessive enzyme deactivation. At dosing rates below 15 µM/h, the H_2O_2 concentration in the reactor remained stable below 0.5 µM as long as an organic substrate was present (SMX, TP1 and TP2) (Fig. S6).

Indeed, as shown in Fig. 6**A**, the stability of the enzyme was significantly improved in a fed-batch experiment with a dosing rate of 23.7 µM/h H_2O_2 and an initial SMX concentration of 50 mg/L (approximately 200 µM) compared to the experiments shown in Fig. 5 (900 µg/L or 4.3 µM). In these experiments, additional reaction products were detected in the HPLC samples (Fig. S8), and in addition, the formation of a yellow precipitate was observed. This is probably the result of azoxy product formation that was recently described to be catalysed

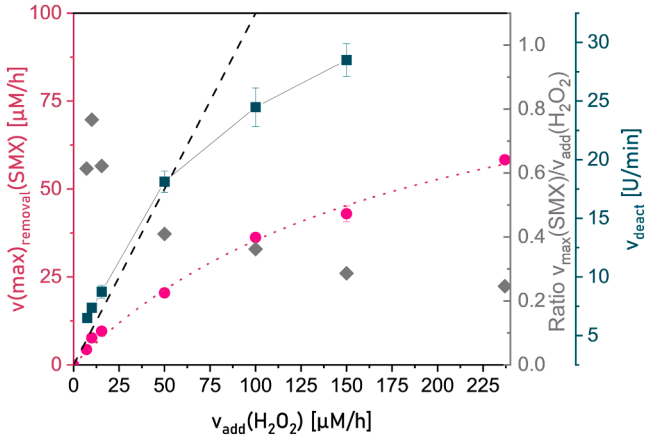

Fig. 5. Pink dots: Maximum SMX removal rate determined at different H_2O_2 dosing rates in fed batch experiments; grey diamonds: H_2O_2 efficiency in terms of the ratio between SMX removal rate and H_2O_2 addition rate, Green squares: apparent enzyme deactivation rates, according to the observed linear decrease in activity in Fig. S6. The dashed line illustrates a hypothetical 1:1 relation between SMX removal rate and H_2O_2 dosing rate.

by *Aae*UPO [49]. Apparently, however, these transformation pathways requires higher substrate concentrations, which are unlikely to occur in real wastewaters. The influence of substrate concentration on the observed transformation product spectrum has also been reported for laccase-catalysed lignin polymerization [58], and should be considered when drawing conclusions from removal studies at high substrate concentrations.

In a second experiment, the effect of an additional SMX spike added just prior to complete SMX removal was investigated (Fig. 6**B**). It was hypothesized that the stability of the enzyme could be prolonged due to the increased availability of SMX. Although the H_2O_2 concentration could be kept stable, a stepwise decrease in activity was observed after the second spike, with subsequent stabilization until the substrate dosed in the second spike was depleted. The results highlight the need for a process design in which the peroxide concentration is dynamically

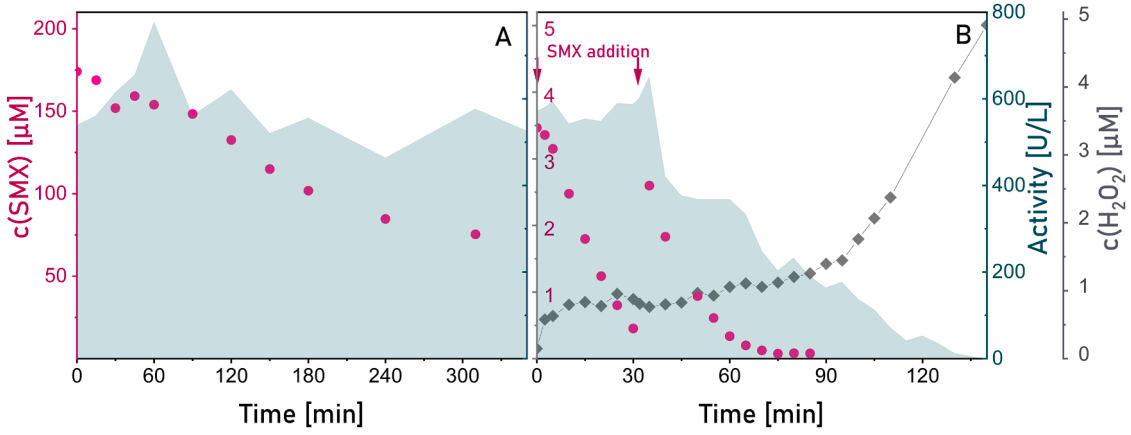

Fig. 6. A) Removal of SMX by *Aae*UPO under a) 23.7 µM/h H_2O_2, 500 U/L *Aae*UPO, 50 mg/L SMX, sodium phosphate buffer pH 7 0.1 M, 22 °C; B) 15.4 µM/h H_2O_2, 500 U/L *Aae*UPO, 900 µg/L SMX in each pulse, deionized water, 22 °C. green: enzyme activity, purple: SMX concentration. Grey: hydrogen peroxide.

adapted to the available substrate concentration and never accumulates in excess over the substrate.

3.4.1. *Continuous operation of AaeUPO in a membrane reactor*

Based on the results obtained in the batch reactor, an enzymatic membrane reactor (EMR) based on a commercial Amicon® stirred cell coupled to a peristaltic pump was operated (Fig. S9). In this configuration, the H_2O_2 feed rate can be adjusted to the substrate concentration present in the reaction mixture. The theoretical and experimental residence times were 85.7 min and 88.6 min, respectively at a flow rate of 2.5 ± 0.1 mL/min, with a characteristic residence time distribution for an ideal continuously stirred tank reactor (CSTR) (Fig. S10). Fig. 7 shows the profiles of SMX removal, enzyme activity and H_2O_2 concentration in three continuous removal experiments at a feed rate of 3.2 ± 0.2 µM/h SMX and different H_2O_2 dosing rates.

At a feed concentration of 42 µM H_2O_2, conversion of more than 95 % SMX could be reached during a period of 150 min. However, the enzyme was deactivated at a rate of 3.4 ± 0.4 U/(L•min), so that a second pulse of fresh enzyme was added after 100 min of operation (Fig. 7**A**). Diminishing the H_2O_2 feed concentration to 20 µM (Fig. 7**B**) had two effects. Firstly, the conversion of SMX was lower, but could be maintained at > 90 % for 150 min without any further enzyme dosing. Secondly, the enzyme deactivation rate could be lowered to 2.7 ± 0.2 U/(L•min). Fig. 7**C** shows that a H_2O_2 feed concentration of 12 µM resulted in an average SMX conversion of 73 ± 4 % over 180 min. Considering the absence (c<0.1 µM) of H_2O_2 in the effluent, the reaction was presumably H_2O_2-limited. Interestingly, SMX removal slightly increased at longer reaction times, accompanied by a shift in the

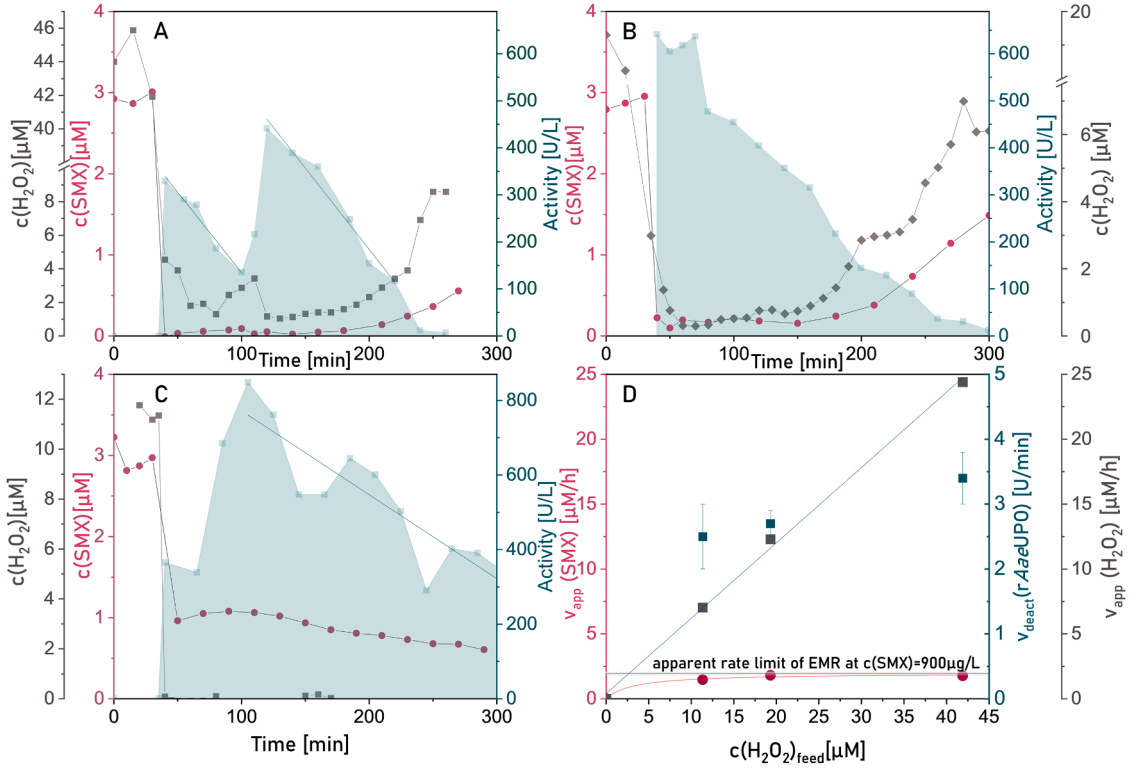

Fig. 7. Concentration of SMX (purple dots), H_2O_2 (grey diamonds) and residual enzyme activity (green area) during continuous removal experiments in deionized water, pH 6 ± 0.5. A) 45 µM H_2O_2 feed, enzyme addition at t = 35 min and t = 105 min B) H_2O_2 µM H_2O_2 feed; enzyme addition at 35 min C) 12 µM H_2O_2 feed; enzyme addition at 35 min D) summary of the apparent reaction rates within the reactor.

occurrence of the additional transformation products (TP1-TP3). This may result from minor conformational changes in the enzyme, altering substrate affinity. Further kinetic studies in the presence of different amounts of the respective transformation products are required to elucidate this relationship. Even at these H_2O_2 limited conditions, the activity of *Aae*UPO dropped by an approximate rate of 2.5 ± 0.5 U/(L•min). Therefore, in addition to heme bleaching caused by excess H_2O_2, other deactivation processes must be occurring. To further narrow down the origin of the enzyme deactivation, additional experiments were performed. The mechanical stability against shear forces in the reactor was monitored by measuring the enzyme stability during three consecutive days while the pump was stopped overnight (Fig. 8**A**).

Apart from some fluctuations due to the interruption of the flow, the enzyme deactivation was considerably slower than in the experiments in the presence of H_2O_2 and SMX (Fig. 7). The flow rate changed only slightly during the experiment, indicating minor effect of fouling. When the enzyme was exposed to an influent H_2O_2 concentration of 20 μM (Fig. 8**B**), the enzyme stability was in fact maintained slightly longer than in presence of SMX (Fig. 7**B**). This apparent contradiction to the stabilising effect of the substrate observed in Fig. 6**A** can be explained by the fact that in the EMR, the H_2O_2 concentration was virtually zero, and instead, the concentration of the products was high. Although no destabilising or inhibiting effect of TP3, 4-nitro-SMX, was observed, previous studies reported that the 4-hydroxylamine SMX intermediate (TP1) can react with structurally similar cytochrome P450 monooxygenases [59]. For peroxidases, the addition of high molecular weight additives as glycerol or polyethylene glycol (PEG) could significantly improve the enzyme mechanical stability and resilience in presence of radicals [60,61]. To explore its potential for *Aae*UPO stabilisation, PEG with a molecular weight of 35000 g/mol was selected. The high molecular weight guarantees its retention by the 10 kDa membrane and prevents it from oxidation by *Aae*UPO [62]. As can be seen in Fig. 8**C**, the addition of PEG (35,000 g/mol) significantly increased the stability of *Aae*UPO during continuous shaking at 22 °C in the absence of H_2O_2 and substrate in batch. However, as shown in Fig. 8**D**, in the continuous operation of the reactor, the addition of 100 mg/L PEG a dosing rate of 20 μM/h H_2O_2 led to no increase of enzyme stability in comparison with the results displayed in Fig. 7**B**. If the formed intermediates contribute to the deactivation, adjusting the residence time could alter their steady-state concentration in the reactor. A decrease in residence time could also increase the apparent SMX removal rate at higher H_2O_2 feed concentrations (Fig. 7**D**). Since in the present configuration the flow rate is limited by the flux across the membrane, either smaller reactor volumes, or immobilisation strategies that allow membrane -free activity retention could be applied [24,63].

3.5. Removal of antibiotic and phytotoxic effect

As complete mineralization of contaminants is typically not achieved by enzymatic pollutant removal strategies, the primary goal is to produce transformation products with decreased environmental effect. However, as discussed in previous studies, this cannot always be achieved [64,65]. An increase in toxicity toward *Daphnia magna* for the sulphonamides sulfadiazine and sulfamethazine had been observed after batch treatment with *Aae*UPO[21]. The authors attribute this to residual H_2O_2 in the reaction effluent. In our work, H_2O_2 does not appear in significant amounts in the treated effluent due to the catalase activity of the enzyme. Therefore, the contribution of metabolites to the observed toxicity cannot be ruled out. Short-term bioassays, such as the standard Microtox assay, which monitors luminescence inhibition in the marine

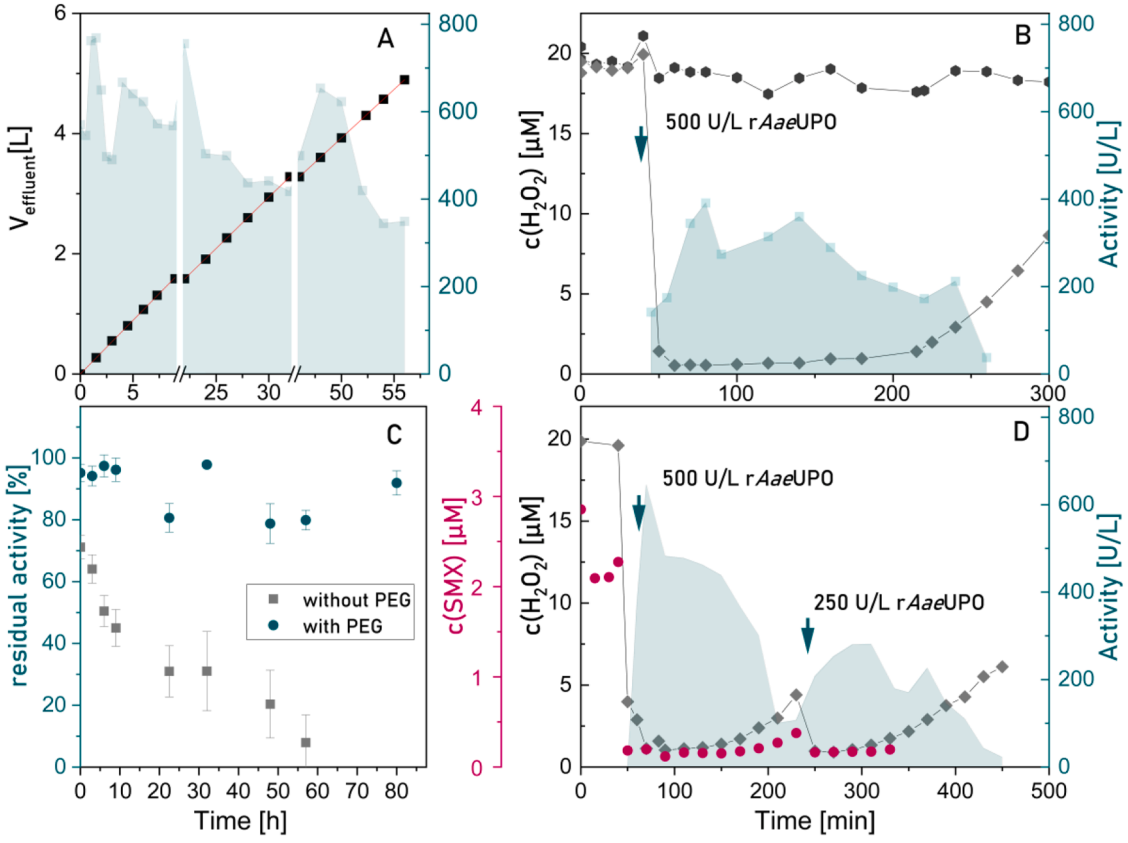

Fig. 8. Stability of *Aae*UPO in different conditions: A) in continuous reactor in the absence of SMX and H_2O_2 B) in continuous reactor at a feed H_2O_2 concentration of 20 μM C) Comparison of *Aae*UPO stability in batch in the presence (green dots) and absence (grey squares) of 400 mg/L PEG D) continuous removal of SMX (purple dots) at a H_2O_2 feed concentration of 20 μM in the presence of 400 mg/L PEG, at 240 min, a second pulse of *Aae*UPO was added to reach a concentration of 250 U/L, grey diamonds represent the H_2O_2 concentration.

microorganism *Aliivibrio fischeri*, are typically less sensitive to bacteriostatic antibiotics like SMX. As a result, more pronounced effects are observed with prolonged incubation times [66,67]. Majewsky et al. [68] compared the two measurement approaches for *A. fischeri* and generally reported higher toxicity for NO_2-SMX than for SMX. Interestingly, in this case, the metabolites had a more pronounced effect on short-term luminescence inhibition than on long-term growth inhibition.

The marine bacterium *A. fischeri* might not be fully representative for the effects on wastewater and freshwater environments. Therefore, the growth inhibition effect on bacteria commonly found in wastewater was assessed. The strain *Escherichia coli K12* exhibited the highest susceptibility to SMX in an agar disk diffusion assay and was thus selected for the broth dilution assay in the presence of treated and untreated spiked water samples. Growth inhibition (I [%]) can be calculated from the ratio of the integrated growth curves at concentration c_x and in the absence of pollutant c_o using Eqn I.

$$I_{exp} = \left(1 - \frac{\int_{t=0}^{t} OD_{600,c_x}}{\int_{t=0}^{t} OD_{600,c_o}}\right) \bullet 100 \quad \text{(I)}$$

Plotting the calculated inhibition percentages against the applied concentrations enables fitting the data to the Hill equation (Eqn II), where the inflection point provides an IC_{50} value of 0.58 mg/L for SMX, with a Hill coefficient of 1.8 ± 0.5 and a coefficient of determination (R^2) of 0.95.

$$I_{fit} = I_0 + \frac{I_{max} \bullet c(Antibiotic)^a}{IC_{50} + c(Antibiotics)^a} \quad \text{(II)}$$

The IC_{50} value for the treated effluent could not be reliably calculated since the applied amount of the concentrated effluent did not reach the maximum inhibitory concentration, but Fig. 9**A** clearly shows a reduction of the growth inhibiting effect.

It should be noted that, due to the relatively high IC_{50} of SMX in this case, at least a tenfold concentrated sample is required to achieve an appropriate ratio with the bacterial broth during the assay. Because of the observed changes in the pattern of transformation products at elevated concentrations, the assay was performed using concentrated effluent.

Concerningly, antibiotics have not only an inhibiting effect on pathogenic bacteria but also on terrestrial plant species [69]. It is expected that the implementation of advanced treatment technologies will be driven not only by stricter regulations but also by increasing water scarcity. Wastewater reuse for irrigation is a likely scenario that must be considered when evaluating the success of a treatment technology. Therefore, the effect of enzymatic treatment of SMX-contaminated water on germination and root length of *Daucus carota* seeds was evaluated (Fig. 9**B**), a species known for its high sensitivity to sulphonamide antibiotics [6].

Based on regulatory standards, a germination index of at least 60 % in the control should be achieved before measuring root length [6]. Compared to the control, germination indices were lower in the presence of both SMX and 4-NO_2-SMX, with the lowest values observed for 4-NO_2-SMX. Interestingly, the average root length after seven days of incubation at two different concentrations of 4-NO_2-SMX was higher than in the corresponding concentrations of SMX, suggesting that enzymatic treatment may reduce phytotoxicity. However, due to the high variance in root length measurements, only a few populations showed significant differences ($p < 0.05$). Unexpectedly, the lower concentrations showed a greater inhibitory effect on both root length and germination index. This can be explained by a hormetic effect, where an organism shows a stimulatory response to increasing concentrations of a stressor, as previously reported for heavy metals and antibiotics [70,71]. The observed variance in root length is largely due to differences in the timing of germination, which could be minimized by continuous monitoring of root elongation rates [72].

3.6. Mixture effects

Even when focusing on a single contaminant, the removal process depends not only on the concentrations of substrates, cosubstrates and enzymes, but also on the transformation products formed. In more realistic scenarios, several antibiotics and other wastewater constituents are likely to be present simultaneously, which could influence the removal kinetics of each. We conducted removal experiments with various combinations of antibiotics under continuous H_2O_2 feeding. Using a H_2O_2 dosing rate of 37 μM/h and an initial antibiotic concentration of 5 mg/L each, SMX degradation reached 100 % within one hour, unaffected by the presence of TMP (Fig. 10**A** and **C**). Conversely, when considering the removal of TMP, in the SMX-TMP mixture, less than 15 % TMP removal was observed after 2 hours, compared to 60 % removal of TMP alone in the same timeframe. Interestingly, in this case,

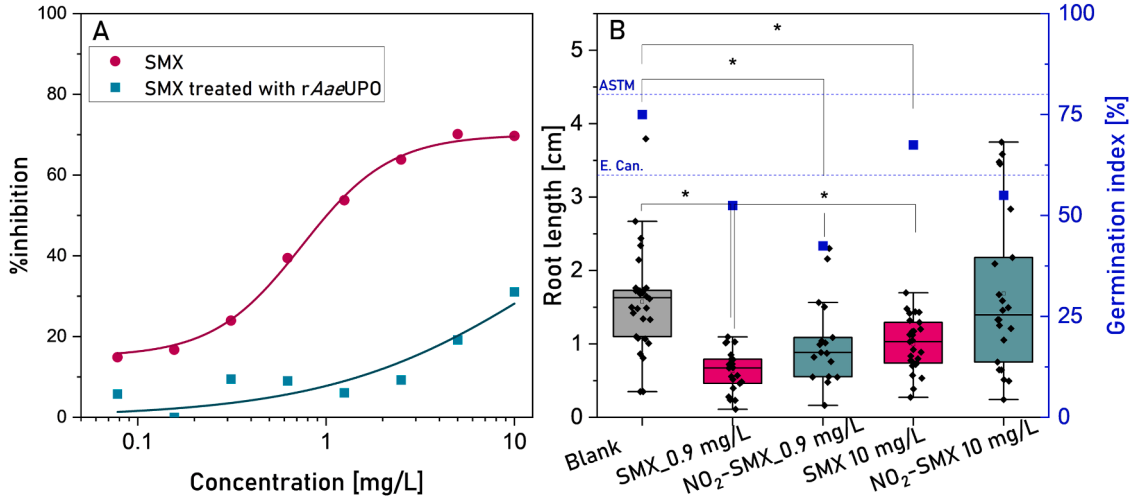

Fig. 9. A) Growth inhibition of E. coli calculated by formula (II). The considered time frame for growth curve comparison ranged from 0 to 2000 s. Data was fitted with the Hill equation. Individual growth curves with standard deviations from biological triplicates can be found in Fig. S11 B) Left Y axis: Root length of D. carota in the presence of different concentrations of SMX and 4-NO_2-SMX after 7 d of incubation. Right Y axis: germination index (blue squares) dashed horizontal lines indicate the minimal germination index of the blank required by the ASTM (American Society for Testing and Materials) and Environment Canada (E. Can.).

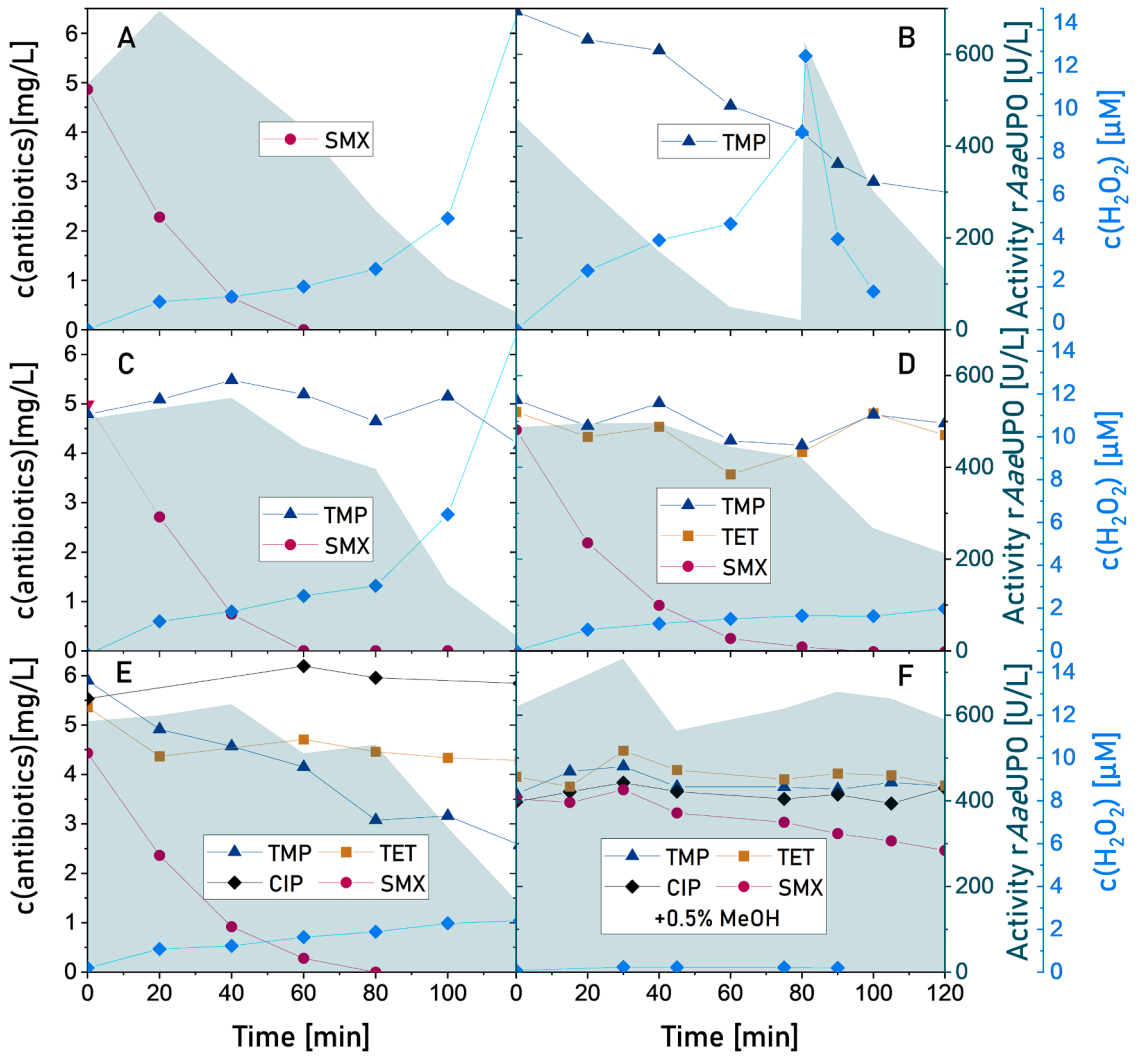

Fig. 10. Removal of antibiotics in different combinations in distilled water; pH 6.5 A) SMX alone B) TMP alone C) Mix of SMX and TMP D) mix of SMX, TMP and TET E) Mix of SMX, TMP, TET and CIP F) Mix of SMX, TMP, TET and CIP in the presence of 0.5 % MeOH. Blue triangles: c(TMP); Black diamonds: c(CIP); Brown squares: c (TET); Pink dots c(SMX); Light blue diamonds: $c(H_2O_2)$; Green shaded area: residual enzyme activity.

a higher rate of enzyme deactivation was observed, demanding the addition of a second pulse of active enzyme after 80 minutes (Fig. 10**B**). The slower removal rate of TMP compared to SMX suggests a lower affinity for binding to Compound I. As a result, when TMP is the only substrate available, enzyme deactivation occurs more rapidly due to a greater proportion of heme bleaching compared to productive substrate conversion.

When TET was also present in the mixture, the removal rate of SMX slightly decreased, while the H_2O_2 concentration remained relatively stable below 2 µM, indicating higher enzyme stability (Fig. 10**D**). In a mixture of the four antibiotics—SMX, TMP, CIP, and TET—the removal of SMX remained unchanged compared to the previous case (Fig. 10**E**). Interestingly, TMP removal was more efficient, while TET and CIP were not removed at all, consistent with the batch experiments shown in Fig. 2. A significant observation was made in the presence of 0.5 % (v/v) methanol (Fig. 10**F**): the removal of the four antibiotics nearly ceased, except for SMX. Meanwhile, enzyme activity remained constant, and no H_2O_2 was detected. It has been demonstrated that methanol is a substrate for *Aae*UPO [73], and in this case, the methanol concentration represents a thousand-fold excess over the applied micropollutant concentration and acts as a competitive inhibitor. To control the solvent used in micropollutant spiking, it is crucial to either use inert alternatives or to evaporate the solvent before adding it to the water matrix. In addition, the stabilizing effect of other natural organic substrates may be an interesting area for further studies on the influence of more complex water matrices.

4. Conclusions

Even though all of the considered antibiotics could be removed by at least one of the applied oxidoreductases, transitioning from laboratory experiments to real-world applications requires considering factors beyond removal efficiency. It is essential to evaluate enzyme functionality under varying process conditions (pH, temperature) to ensure compatibility with real wastewater. In this regard, despite its broader substrate scope and higher stability, *Ci*VCPO failed to remove the target antibiotics in WWTP effluentr, highlighting the need for further investigation into inhibition mechanisms. While *Aae*UPO remained active in wastewater, fed-batch studies revealed the challenge of optimising the H_2O_2 dosing rate to minimise the unproductive catalase mechanism at low substrate concentrations. To further assess its feasibility, a continuous system was operated to enhance the catalytic performance of the biocatalyst. An enzyme dose of 500 U/L successfully removed over 90 % of SMX within 150 minutes before additional enzyme dosing was required. The desired removal efficiency could be further adjusted based on the H_2O_2 feed provided. Future work should focus on implementing

an appropriate control system for H_2O_2 and enzyme dosing, depending on the pollutant concentration in the feed, to improve process stability. In addition, mutual inhibition effects in more complex substrate matrices were observed and need to be considered for practical applications. While this study focused on evaluating the technological challenges of enzymatic treatment, the widespread adoption of enzyme-based treatment technologies will ultimately depend on their economic competitiveness with existing treatment processes. Although the studied enzymes are not yet economically on par with established large-scale processes, advancements such as increased expression levels in heterologous hosts, simplified downstream processing, and enhanced stability through enzyme engineering and suitable immobilization techniques may change this in the future.

CRediT authorship contribution statement

Schäffer Andreas: Writing – review & editing, Supervision, Project administration, Funding acquisition. **Moreira María Teresa:** Writing – review & editing, Supervision, Resources, Project administration, Funding acquisition. **de Boer Sabrina:** Writing – original draft, Visualization, Methodology, Investigation, Formal analysis, Data curation, Conceptualization. **Sastre Daniel:** Writing – review & editing, Investigation. **Hollmann Frank:** Writing – review & editing, Visualization, Resources. **Lores Marta:** Writing – review & editing, Resources. **Castillo Aly:** Writing – review & editing, Investigation, Formal analysis, Data curation. **Méndez Sabela Balboa:** Resources, Investigation, Formal analysis.

Declaration of Competing Interest

The authors declare that they have no known competing financial interests or personal relationships that could have appeared to influence the work reported in this paper.

Acknowledgements

This study was funded by the European Union's Horizon 2020 research and innovation program under the Marie Sklodowska-Curie grant agreement No 812880 and by CIES (PID2022–142334OB-I00) project granted by MCIN-AEI and the Spanish Ministry of Science and Innovation. The authors would like to thank Dr. Martin Krauss (UFZ) for his help provided during identification of transformation products.

Appendix A. Supporting information

Supplementary data associated with this article can be found in the online version at doi:10.1016/j.jece.2025.115795.

Data availability

Data will be made available on request.

References

[1] M. Rodell, J.S. Famiglietti, D.N. Wiese, J.T. Reager, H.K. Beaudoing, F.W. Landerer, M.H. Lo, Emerging trends in global freshwater availability, Nature 557 (2018) 651–659, https://doi.org/10.1038/s41586-018-0123-1.
[2] EEA, European Waters, 2018. ISBN: 978-92-9213-947-6.
[3] N.H. Tran, H. Chen, M. Reinhard, F. Mao, K.Y.-H. Gin, Occurrence and removal of multiple classes of antibiotics and antimicrobial agents in biological wastewater treatment processes, Water Res. 104 (2016) 461–472, https://doi.org/10.1016/j.watres.2016.08.040.
[4] L. Rizzo, C. Manaia, C. Merlin, T. Schwartz, C. Dagot, M.C. Ploy, I. Michael, D. Fatta-Kassinos, Urban wastewater treatment plants as hotspots for antibiotic resistant bacteria and genes spread into the environment: a review, Sci. Total Environ. 447 (2013) 345–360, https://doi.org/10.1016/j.scitotenv.2013.01.032.
[5] N.A. Sabri, S. van Holst, H. Schmitt, B.M. van der Zaan, H.W. Gerritsen, H.H. M. Rijnaarts, A.A.M. Langenhoff, Fate of antibiotics and antibiotic resistance genes during conventional and additional treatment technologies in wastewater treatment plants, Sci. Total Environ. 741 (2020), https://doi.org/10.1016/j.scitotenv.2020.140199.
[6] D.G. Hillis, J. Fletcher, K.R. Solomon, P.K. Sibley, Effects of ten antibiotics on seed germination and root elongation in three plant species, Arch. Environ. Contam. Toxicol. 60 (2011) 220–232, https://doi.org/10.1007/s00244-010-9624-0.
[7] S. de Boer, J. González-Rodríguez, J.J. Conde, M.T. Moreira, Benchmarking tertiary water treatments for the removal of micropollutants and pathogens based on operational and sustainability criteria, J. Water Process Eng. 46 (2022) 102587, https://doi.org/10.1016/j.jwpe.2022.102587.
[8] T. Brugnari, D.M. Braga, C.S.A. dos Santos, B.H.C. Torres, T.A. Modkovski, C.W. I. Haminiuk, G.M. Maciel, Laccases as green and versatile biocatalysts: from lab to enzyme market—an overview, Bioresour. Bioprocess. 8 (2021) 131, https://doi.org/10.1186/s40643-021-00484-1.
[9] C.A. Gasser, E.M. Ammann, P. Shahgaldian, P.F.-X. Corvini, Laccases to take on the challenge of emerging organic contaminants in wastewater, Appl. Microbiol. Biotechnol. 98 (2014) 9931–9952, https://doi.org/10.1007/s00253-014-6177-6.
[10] D. Schlosser, Laccases in Bioremediation and Waste Valorisation, Springer Nature, Cham, Switzerland, 2020, https://doi.org/10.1007/978-3-030-47906-0.
[11] F. Xu, J.J. Kulys, K. Duke, K. Li, K. Krikstopaitis, H.-J.W. Deussen, E. Abbate, V. Galinyte, P. Schneider, Redox chemistry in laccase-catalyzed oxidation of N-hydroxy compounds, Appl. Environ. Microbiol. 66 (2000) 2052–2056, https://doi.org/10.1128/AEM.66.5.2052-2056.2000.
[12] B. Varga, V. Somogyi, M. Meiczinger, N. Kováts, E. Domokos, Enzymatic treatment and subsequent toxicity of organic micropollutants using oxidoreductases - a review, J. Clean. Prod. 221 (2019) 306–322, https://doi.org/10.1016/j.jclepro.2019.02.135.
[13] P. Molina-Espeja, E. Garcia-Ruiz, D. Gonzalez-Perez, R. Ullrich, M. Hofrichter, M. Alcalde, Directed evolution of unspecific peroxygenase from Agrocybe aegerita, Appl. Environ. Microbiol. 80 (2014) 3496–3507, https://doi.org/10.1128/AEM.00490-14.
[14] P. Molina-Espeja, S. Ma, D.M. Mate, R. Ludwig, M. Alcalde, Tandem-yeast expression system for engineering and producing unspecific peroxygenase, Enzym. Microb. Technol. 73–74 (2015) 29–33, https://doi.org/10.1016/j.enzmictec.2015.03.004.
[15] R. Ullrich, J. Nüske, K. Scheibner, J. Spantzel, M. Hofrichter, J. Nuske, K. Scheibner, J. Spantzel, M. Hofrichter, Novel haloperoxidase from the agaric basidiomycete agrocybe aegerita oxidizes aryl alcohols and aldehydes, Appl. Environ. Microbiol. 70 (2004) 4575–4581, https://doi.org/10.1128/AEM.70.8.4575-4581.2004.
[16] J.W.P.M. van Schijndel, E.G.M. Vollenbroek, R. Wever, The chloroperoxidase from the fungus Curvularia inaequalis; a novel vanadium enzyme, Biochim. Biophys. Acta - Protein Struct. Mol. Enzymol. 1161 (1993) 249–256, https://doi.org/10.1016/0167-4838(93)90221-C.
[17] D.T. Monterrey, A. Menés-Rubio, M. Keser, D. Gonzalez-Perez, M. Alcalde, Unspecific peroxygenases: the pot of gold at the end of the oxyfunctionalization rainbow? Curr. Opin. Green Sustain. Chem. 41 (2023) 100786 https://doi.org/10.1016/j.cogsc.2023.100786.
[18] A. Beltrán-Nogal, I. Sánchez-Moreno, D. Méndez-Sánchez, P. Gómez de Santos, F. Hollmann, M. Alcalde, Surfing the wave of oxyfunctionalization chemistry by engineering fungal unspecific peroxygenases, Curr. Opin. Struct. Biol. 73 (2022) 102342, https://doi.org/10.1016/j.sbi.2022.102342.
[19] A. Karich, R. Ullrich, K. Scheibner, M. Hofrichter, Fungal unspecific peroxygenases oxidize the majority of organic EPA priority pollutants, Front. Microbiol. 8 (2017), https://doi.org/10.3389/fmicb.2017.01463.
[20] M. Poraj-Kobielska, M. Kinne, R. Ullrich, K. Scheibner, G. Kayser, K.E. Hammel, M. Hofrichter, Preparation of human drug metabolites using fungal peroxygenases, Biochem. Pharmacol. 82 (2011) 789–796, https://doi.org/10.1016/j.bcp.2011.06.020.
[21] N. Lemańska, E. Felis, M. Poraj-Kobielska, Z. Gajda-Meissner, M. Hofrichter, Comparison of sulphonamides decomposition efficiency in ozonation and enzymatic oxidation processes, Arch. Environ. Prot. 47 (2021) 10–18, https://doi.org/10.24425/aep.2021.136443.
[22] A. Karich, K. Scheibner, R. Ullrich, M. Hofrichter, Exploring the catalase activity of unspecific peroxygenases and the mechanism of peroxide-dependent heme destruction, J. Mol. Catal. B Enzym. 134 (2016) 238–246, https://doi.org/10.1016/j.molcatb.2016.10.014.
[23] S. Bormann, D. Hertweck, S. Schneider, J.Z. Bloh, R. Ulber, A.C. Spiess, D. Holtmann, Modeling and simulation-based design of electroenzymatic batch processes catalyzed by unspecific peroxygenase from A. aegerita, Biotechnol. Bioeng. 118 (2021) 7–16, https://doi.org/10.1002/bit.27545.
[24] L.-E. Meyer, B. Fogtmann Hauge, T. Müller Kvorning, P. De Santis, S. Kara, Continuous oxyfunctionalizations catalyzed by unspecific peroxygenase, Catal. Sci. Technol. 12 (2022) 6473–6485, https://doi.org/10.1039/D2CY00650B.
[25] H.B. ten Brink, H.L. Dekker, H.E. Schoemaker, R. Wever, Oxidation reactions catalyzed by vanadium chloroperoxidase from Curvularia inaequalis, J. Inorg. Biochem. 80 (2000) 91–98, https://doi.org/10.1016/S0162-0134(00)00044-1.
[26] R. Renirie, C. Pierlot, R. Wever, J.-M. Aubry, Singlet oxygenation in microemulsion catalysed by vanadium chloroperoxidase, J. Mol. Catal. B Enzym. 56 (2009) 259–264, https://doi.org/10.1016/j.molcatb.2008.05.014.
[27] T.P. Van Boeckel, S. Gandra, A. Ashok, Q. Caudron, B.T. Grenfell, S.A. Levin, R. Laxminarayan, Global antibiotic consumption 2000 to 2010: an analysis of national pharmaceutical sales data, Lancet Infect. Dis. 14 (2014) 742–750, https://doi.org/10.1016/S1473-3099(14)70780-7.
[28] A.C. Reis, B.A. Kolvenbach, O.C. Nunes, P.F.X. Corvini, Biodegradation of antibiotics: The new resistance determinants – part II, New Biotechnol. 54 (2020) 13–27, https://doi.org/10.1016/j.nbt.2019.08.003.

[29] R. Loos, S. Daouk, D. Marinov, L. Gómez, E. Porcel-Rodríguez, I. Sanseverino, L. Amalric, M. Potalivo, E. Calabretta, M. Ferenčík, L. Colzani, L. DellaVedova, L. Amendola, M. Saurini, F. Di Girolamo, S. Lardy-Fontan, M. Sengl, U. Kunkel, O. Svahn, S. Weiss, S. De Martin, V. Gelao, M. Bazzichetto, P. Tarábek, D. Stipaničev, S. Repec, D. Zacs, M. Ricci, O. Golovko, C. Flores, S. Ramani, R. Rebane, J.A. Rodríguez, T. Lettieri, Summary recommendations on "Analytical methods for substances in the Watch List under the Water Framework Directive, Sci. Total Environ. 912 (2024) 168707, https://doi.org/10.1016/j.scitotenv.2023.168707.

[30] S.R. de Boer, A. Schäffer, M.T. Moreira, Towards oxidoreductase-based processes for the removal of antibiotics from wastewater, Rev. Environ. Sci. Biol./Technol. 22 (2023) 899–932, https://doi.org/10.1007/s11157-023-09676-x.

[31] G.T. Höfler, A. But, S.H.H. Younes, R. Wever, C.E. Paul, I.W.C.E. Arends, F. Hollmann, Chemoenzymatic halocyclization of 4-pentenoic acid at preparative scale, ACS Sustain. Chem. Eng. 8 (2020) 2602–2607, https://doi.org/10.1021/acssuschemeng.9b07494.

[32] R. Wever, R. Renirie, F. Hollmann, Vanadium chloroperoxidases as versatile biocatalysts. Vanadium Catal, The Royal Society of Chemistry, 2020, pp. 548–563, 10.1039/9781839160882-00548.

[33] E. de Boer, H. Plat, M.G.M. Tromp, R. Wever, M.C.R. Franssen, H.C. van der Plas, E. M. Meijer, H.E. Schoemaker, Vanadium containing bromoperoxidase: an example of an oxidoreductase with high operational stability in aqueous and organic media, Biotechnol. Bioeng. 30 (1987) 607–610, https://doi.org/10.1002/bit.260300504.

[34] A. Castillo, S. Pereira, A. Otero, S. Fiol, C. Garcia-Jares, M. Lores, Matrix solid-phase dispersion as a greener alternative to obtain bioactive extracts from Haematococcus pluvialis. Characterization by UHPLC-QToF, RSC Adv. 10 (2020) 27995–28006, https://doi.org/10.1039/D0RA04378H.

[35] Z.Y. Jiang, A.C.S. Woollard, S.P. Wolff, Hydrogen peroxide production during experimental protein glycation, FEBS Lett. 268 (1990) 69–71, https://doi.org/10.1016/0014-5793(90)80974-N.

[36] A. Imbrogno, H.Y. Lin, B. Minofar, A.I. Schäfer, Nanofiber composite ultrafiltration membrane functionalized with cross-linked β-cyclodextrin for steroid hormone micropollutant removal, J. Memb. Sci. 691 (2024) 122212, https://doi.org/10.1016/j.memsci.2023.122212.

[37] C.A. Schneider, W.S. Rasband, K.W. Eliceiri, NIH Image to ImageJ: 25 years of image analysis, Nat. Methods 9 (2012) 671–675, https://doi.org/10.1038/nmeth.2089.

[38] G. Strukul (Ed.), Catalytic Oxidations with Hydrogen Peroxide as Oxidant, Springer Netherlands, Dordrecht, 1992, https://doi.org/10.1007/978-94-017-0984-2.

[39] A. Butler, Mechanistic considerations of the vanadium haloperoxidases, Coord. Chem. Rev. 187 (1999) 17–35, https://doi.org/10.1016/S0010-8545(99)00033-8.

[40] X.-Z. Niu, F. Busetti, M. Langsa, J.-P. Croué, Roles of singlet oxygen and dissolved organic matter in self-sensitized photo-oxidation of antibiotic norfloxacin under sunlight irradiation, Water Res. 106 (2016) 214–222, https://doi.org/10.1016/j.watres.2016.10.002.

[41] X. Luo, Z. Zheng, J. Greaves, W.J. Cooper, W. Song, Trimethoprim: Kinetic and mechanistic considerations in photochemical environmental fate and AOP treatment, Water Res. 46 (2012) 1327–1336, https://doi.org/10.1016/j.watres.2011.12.052.

[42] G. Dedola, E. Fasani, A. Albini, The photoreactions of trimethoprim in solution, J. Photochem. Photobiol. A Chem. 123 (1999) 47–51, https://doi.org/10.1016/S1010-6030(99)00047-7.

[43] M. Kinne, M. Poraj-Kobielska, S.A. Ralph, R. Ullrich, M. Hofrichter, K.E. Hammel, Oxidative cleavage of diverse ethers by an extracellular fungal peroxygenase, J. Biol. Chem. 284 (2009) 29343–29349, https://doi.org/10.1074/jbc.M109.040857.

[44] R. Mireles, J. Ramirez-Ramirez, M. Alcalde, M. Ayala, Ether oxidation by an evolved fungal heme-peroxygenase: insights into substrate recognition and reactivity, J. Fungi 7 (2021), https://doi.org/10.3390/jof7080608.

[45] M. Hofrichter, H. Kellner, R. Herzog, A. Karich, C. Liers, K. Scheibner, V.W. Kimani, R. Ullrich, Fungal peroxygenases: a phylogenetically old superfamily of heme enzymes with promiscuity for Oxygen Transfer Reactions, Gd. Chall. Biol. Biotechnol. (2020) 369–403, https://doi.org/10.1007/978-3-030-29541-7_14.

[46] Y. Ding, K. Cui, Z. Guo, M. Cui, Y. Chen, Manganese peroxidase mediated oxidation of sulfamethoxazole: Integrating the computational analysis to reveal the reaction kinetics, mechanistic insights, and oxidation pathway, J. Hazard. Mater. 415 (2021) 125719, https://doi.org/10.1016/j.jhazmat.2021.125719.

[47] G. Bairán, E. Chávez-Bravo, J. Ortiz-Álvarez, C. Romero-Guido, E. Torres, Oxidation of sulfonamide micropollutants by versatile peroxidase from Bjerkandera adusta, Rev. Int. Contam. Ambient. 38 (2022) 391–405, https://doi.org/10.20937/RICA.54390.

[48] R. Ullrich, C. Dolge, M. Kluge, M. Hofrichter, Pyridine as novel substrate for regioselective oxygenation with aromatic peroxygenase from Agrocybe aegerita, FEBS Lett. 582 (2008) 4100–4106, https://doi.org/10.1016/j.febslet.2008.11.006.

[49] W. Zhang, H. Li, Y. Huang, F. Chen, Z. Zeng, F. Hollmann, X. Wu, X. Zhang, P. Duan, H. Su, J. Shi, X. Sheng, W. Zhang, Unspecific peroxygenase enabled formation of azoxy compounds, Nat. Commun. 15 (2024) 8312, https://doi.org/10.1038/s41467-024-52648-0.

[50] N. Tanaka, R. Wever, Inhibition of vanadium chloroperoxidase from the fungus Curvularia inaequalis by hydroxylamine, hydrazine and azide and inactivation by phosphate, J. Inorg. Biochem. 98 (2004) 625–631, https://doi.org/10.1016/j.jinorgbio.2004.02.001.

[51] J.W.P.M. Van Schijndel, P. Barnett, J. Roelse, E.G.M. Vollenbroek, R. Wever, The stability and steady-state kinetics of vanadium chloroperoxidase from the fungus curvularia inaequalis, Eur. J. Biochem. 225 (1994) 151–157, https://doi.org/10.1111/j.1432-1033.1994.00151.x.

[52] L. Wiest, T. Chonova, A. Bergé, R. Baudot, F. Bessueille-Barbier, L. Ayouni-Derouiche, E. Vulliet, Two-year survey of specific hospital wastewater treatment and its impact on pharmaceutical discharges, Environ. Sci. Pollut. Res. 25 (2018) 9207–9218, https://doi.org/10.1007/s11356-017-9662-5.

[53] M.P. Wilson, F. Worrall, The heat recovery potential of "wastewater": a national analysis of sewage effluent discharge temperatures, Environ. Sci. Water Res. Technol. 7 (2021) 1760–1777, https://doi.org/10.1039/d1ew00411e.

[54] M. Zeyadi, Y.Q. Almulaiky, A novel peroxidase from Ziziphus jujuba fruit: purification, thermodynamics and biochemical characterization properties, Sci. Rep. 10 (2020) 1–12, https://doi.org/10.1038/s41598-020-64599-9.

[55] J.M. Steinweg, S. Jagadamma, J. Frerichs, M.A. Mayes, Activation energy of extracellular enzymes in soils from different biomes, PLoS One 8 (2013) e59943, https://doi.org/10.1371/journal.pone.0059943.

[56] L.F. Stadlmair, T. Letzel, J. Graßmann, Monitoring enzymatic degradation of emerging contaminants using a chip-based robotic nano-ESI-MS tool, Anal. Bioanal. Chem. 410 (2018) 27–32, https://doi.org/10.1007/s00216-017-0729-4.

[57] K. Hernandez, A. Berenguer-Murcia, R. C. Rodrigues, R. Fernandez-Lafuente, Hydrogen peroxide in biocatalysis. a dangerous liaison, Curr. Org. Chem. 16 (2012) 2652–2672, https://doi.org/10.2174/138527212804004526.

[58] D. Areskogh, J. Li, G. Gellerstedt, G. Henriksson, Investigation of the molecular weight increase of commercial lignosulfonates by laccase catalysis, Biomacromolecules 11 (2010) 904–910, https://doi.org/10.1021/bm901258v.

[59] A.E. Cribb, S.P. Spielberg, G.P. Griffin, N4-hydroxylation of sulfamethoxazole by cytochrome P450 of the cytochrome P4502C subfamily and reduction of sulfamethoxazole hydroxylamine in human and rat hepatic microsomes, Drug Metab. Dispos. 23 (1995) 406–414. PMID:1686233.

[60] S. Nakamoto, N. Machida, Phenol removal from aqueous solutions by peroxidase-catalyzed reaction using additives, Water Res. 26 (1992) 49–54, https://doi.org/10.1016/0043-1354(92)90110-P.

[61] I.D. Buchanan, J.A. Nicell, Kinetics of peroxidase interactions in the presence of a protective additive, J. Chem. Technol. Biotechnol. 72 (1999) 23–32, https://doi.org/10.1002/(SICI)1097-4660(199805)72:1< 23::AID-JCTB867> 3.0.CO;2-N.

[62] M. Kinne, The extracellular peroxygenase of the agaric fungus Agrocybe aegerita: catalytic properties and physiological background with particular emphasis on ether cleavage, Int. Hochschulinstitut Zittau (2010).

[63] M. Hobisch, P. De Santis, S. Serban, A. Basso, E. Byström, S. Kara, Peroxygenase-driven ethylbenzene hydroxylation in a rotating bed reactor, Org. Process Res. Dev. 26 (2022) 2761–2765, https://doi.org/10.1021/acs.oprd.2c00211.

[64] M. Bilal, S.S. Ashraf, D. Barceló, H.M.N. Iqbal, Biocatalytic degradation/redefining "removal" fate of pharmaceutically active compounds and antibiotics in the aquatic environment, Sci. Total Environ. 691 (2019) 1190–1211, https://doi.org/10.1016/j.scitotenv.2019.07.224.

[65] D. Becker, S. Varela Della Giustina, S. Rodriguez-Mozaz, R. Schoevaart, D. Barceló, M. de Cazes, M.P. Belleville, J. Sanchez-Marcano, J. de Gunzburg, O. Couillerot, J. Völker, J. Oehlmann, M. Wagner, Removal of antibiotics in wastewater by enzymatic treatment with fungal laccase – degradation of compounds does not always eliminate toxicity, Bioresour. Technol. 219 (2016) 500–509, https://doi.org/10.1016/j.biortech.2016.08.004.

[66] B.I. Escher, A. Baumer, K. Bittermann, L. Henneberger, M. König, C. Kühnert, N. Klüver, General baseline toxicity QSAR for nonpolar, polar and ionisable chemicals and their mixtures in the bioluminescence inhibition assay with Aliivibrio fischeri, Environ. Sci. Process. Impacts 19 (2017) 414–428, https://doi.org/10.1039/C6EM00692B.

[67] T. Backhaus, L.H. Grimme, The toxicity of antibiotic agents to the luminescent bacterium Vibrio fischeri, Chemosphere 38 (1999) 3291–3301, https://doi.org/10.1016/S0045-6535(98)00560-8.

[68] M. Majewsky, D. Wagner, M. Delay, S. Bräse, V. Yargeau, H. Horn, Antibacterial activity of sulfamethoxazole transformation products (TPs): general relevance for sulfonamide TPs modified at the para Position, Chem. Res. Toxicol. 27 (2014) 1821–1828, https://doi.org/10.1021/tx500267x.

[69] M. Carballo, A. Rodríguez, A. de la Torre, Phytotoxic effects of antibiotics on terrestrial crop plants and wild plants: a systematic review, Arch. Environ. Contam. Toxicol. 82 (2022) 48–61, https://doi.org/10.1007/s00244-021-00893-5.

[70] D. Yang, Z. Guo, I.D. Green, D. Xie, Effect of cadmium accumulation on mineral nutrient levels in vegetable crops: potential implications for human health, Environ. Sci. Pollut. Res. 23 (2016) 19744–19753, https://doi.org/10.1007/s11356-016-7186-z.

[71] L. Migliore, A. Rotini, N.L. Cerioli, S. Cozzolino, M. Fiori, Phytotoxic antibiotic sulfadimethoxine elicits a complex hormetic response in the weed Lythrum salicaria L, Dose-Response 8 (2010), https://doi.org/10.2203/dose-response.09-033.Migliore.

[72] N. Yazdanbakhsh, J. Fisahn, Analysis of Arabidopsis thaliana root growth kinetics with high temporal and spatial resolution, Ann. Bot. 105 (2010) 783–791, https://doi.org/10.1093/aob/mcq048.

[73] T. Hilberath, A. van Troost, M. Alcalde, F. Hollmann, Assessing peroxygenase-mediated oxidations in the presence of high concentrations of water-miscible co-solvents, Front. Catal. 2 (2022), https://doi.org/10.3389/fctls.2022.882992.